



Formation of coating and tribological behavior of kinetic sprayed Fe-based bulk metallic glass

Sanghoon Yoon^a, Junghwan Kim^a, Gyuyeol Bae^a, Byungdoo Kim^b, Changhee Lee^{a,*}

^a Kinetic Spraying Coating Laboratory (NRL), Division of Materials Science and Engineering, Hanyang University, 17 Haengdang-dong, Seongdong-gu, Seoul 133-791, Republic of Korea

^b Hankook Coatings, Asan 195-32, Chungnam, Republic of Korea

ARTICLE INFO

Article history:

Received 17 May 2010

Received in revised form 31 August 2010

Accepted 3 September 2010

Available online 21 September 2010

Keywords:

Fe-based bulk metallic glass (BMG)

Kinetic (or cold) spraying

Dense coating

Tribological behavior

Wear resistance

ABSTRACT

Fe-based bulk metallic glass (BMG) was sprayed through the kinetic spraying process using different conditions. By using helium as the process gas and a preheating system for the powder, it was possible to form a dense coating. This study focused on the deposition characteristics and tribological behavior of Fe-based BMG coating in comparison to the bearing materials (bearing steel and steel-backed sintered bearing) for industrial applications. Observations of the worn surface of the coating revealed that the plastic deformation with grooves and some debris were prominent with no visible cracking or fracture. Fe-based BMG coating showed a good wear resistance with a low friction coefficient.

© 2010 Elsevier B.V. All rights reserved.

1. Introduction

Owing to their unique properties, such as mechanical/thermomechanical properties and electrochemical properties, bulk metallic glass (BMG) materials have been drawing attention in the engineering field [1,2]. Especially, Fe-based BMG has attracted a lot of attention, because this material has extremely high strength, superior corrosion/wear resistance, good magnetic properties, and relatively low material cost for industrial applications [3–5]. All of these properties make the Fe-based BMG a potential engineering material in a range of applications.

In the previous work [6], BMG feedstock was sprayed using thermal spraying processes, such as atmospheric plasma spraying. The in-flight particle melting state and in-flight particle oxidation degree were the critical factors for each process, in view of the amorphous phase fraction in the as-sprayed coatings. Accordingly, thermal and chemical instabilities of the amorphous materials resulting from the process characteristics are considered to be critical points in the thermal spraying process. On the other hand, in the kinetic spraying process, the feedstock is accelerated by the momentum transfer from the cold gas dynamics. As a feedstock is harder to deposit, the critical particle velocity is also higher [7]. Based on the gas dynamics in the nozzle used for kinetic

spraying, the particle temperature is quite low and less than the process gas temperature normally heated to ~600 °C [8]. Moreover, the kinetic spraying process can be considered to be a useful technology for the application of materials showing a high sensitivity to the thermally activated processes [9]. In this study, the Fe-based BMG was sprayed using the kinetic spraying process. BMG material shows limited plasticity below the glass transition temperature [9,10]. Thus, a typical kinetic spraying system (KINETICS 3000, CGT, Germany) was modified with an additional powder preheater [11,12] in order to increase the deposition efficiency of the metallic feedstock with consideration for thermal softening.

This study has focused mainly on the deposition characteristics and tribological behavior of Fe-based BMG coating in comparison to the bearing steel and SBS (steel-backed sintered) bearing [13] for industrial applications. Friction and wear experiments were performed under dry conditions using a pin-on-disk sliding wear test against SUJ2 counter material. The Fe-based BMG coating showed a good wear resistance with a low friction coefficient.

2. Experimental procedures

Fe_{68.8}C_{7.0}Si_{3.5}B_{5.0}P_{9.6}Cr_{2.1}Mo_{2.0}Al_{2.0} (at.%) was manufactured using inert gas atomization [14]. As-received feedstock with a size distribution of +5–90 μm was sieved to +5–45 μm before spraying. Characterization of feedstock material was then conducted using a scanning electron microscopy (revealing the powder morphology as spherical in shape), X-ray diffraction (showing amorphous structure), and differential scanning calorimetry (indicating $T_g = 539$ °C, $T_x = 580$ °C, and $T_m = 1150$ °C), as shown in Fig. 1.

* Corresponding author. Tel.: +82 2 2220 0388; fax: +82 2 2299 0389.
E-mail address: chlee@hanyang.ac.kr (C. Lee).

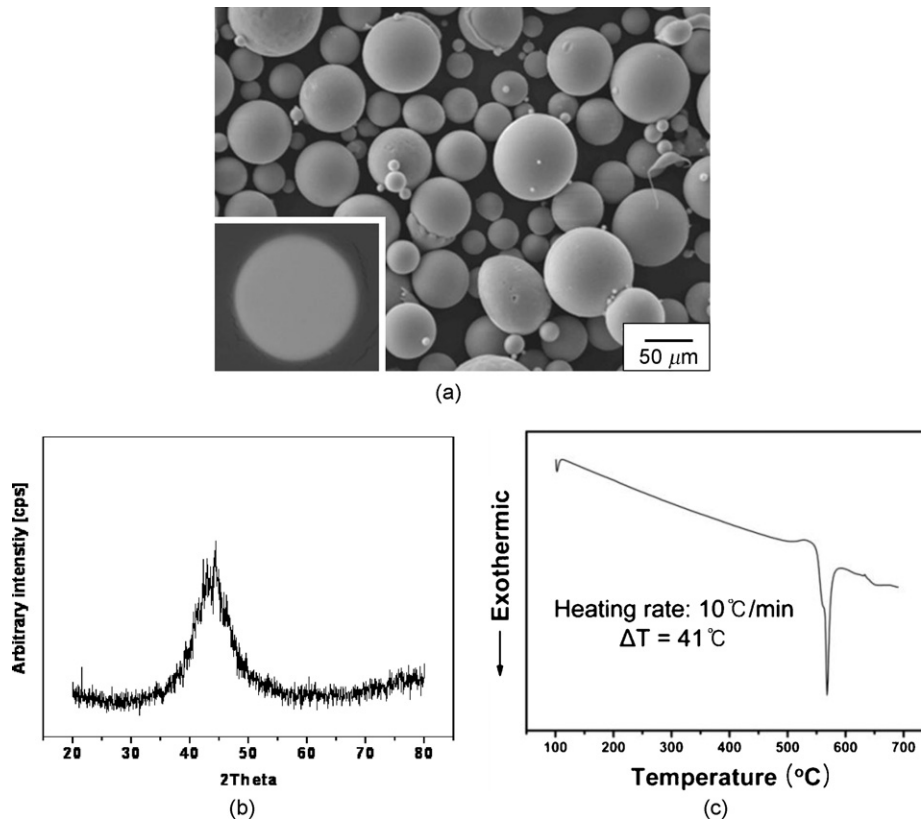


Fig. 1. Characteristics of the feedstocks: (a) morphology of Fe-based BMG, (b) XRD patterns, and (c) DSC curves.

A commercial kinetic spray system was utilized to perform an individual particle impact test and full coating formation at a spray distance of 30 mm. Two different gun traverse speeds of 50 mm/s (used for the full coating formation) and 600 mm/s (used for the individual particle impact test) were adopted. An individual particle impact test was performed to find out whether deposition was possible. To obtain superplastic deformation upon impact, the Fe-based BMG powder was preheated to $\sim 570^\circ\text{C}$, such that it was within the supercooled liquid region (between the glass transition T_g and crystallization T_x temperatures) prior to spraying. The detailed process parameters utilized in this study are shown in Tables 1 and 2.

The microstructure of the coatings was evaluated by scanning electron microscopy (SEM). Friction and wear experiments were performed under dry conditions using a pin-on-disk sliding wear test against SUJ2 ($\text{Fe}_{96.8}\text{C}_{1.04}\text{Si}_{0.28}\text{Mn}_{0.31}\text{Cr}_{1.54}$ (wt.%)) countermaterial for BMG coating, a bearing steel, and a steel-backed sintered (SBS) bearing. The SBS bearing is an oil-less bearing in which a sintered layer made from special Fe–Cu alloy with dispersed MoS_2 is impregnated [13]. Prior to the wear tests, square samples (30 mm \times 30 mm in dimension) were prepared under the same conditions. The surfaces of the samples were mirror polished to a $0.3\text{ }\mu\text{m}$ alumina finish before the tests. A schematic of the pin-on-disk dry sliding wear system and detailed wear parameters are shown in Fig. 2 and Table 3. The microstructure of the worn surfaces was investigated using SEM, followed by the wear test.

3. Results and discussion

3.1. Individual particle impact test

As shown in Fig. 3, the impact behavior of Fe-based BMG was different depending on the processing conditions. Individual particles impacted onto mild steel substrate and a single particle deposition could be obtained. Besides the bonded particles, numerous craters were distributed on the substrate surface. When nitrogen was used as the process gas, most of impacted particles were not bonded onto the substrate even though the process gas was under high pressure and temperature (2.9 MPa and 550°C). From the general viewpoint of particle deposition in the kinetic spraying, the impacting par-

ticle velocity was less than the critical velocity when the particles were accelerated using nitrogen gas. On the other hand, the particle was successfully deposited when the process gas was changed to helium, as can be seen in Fig. 3c and d. As the process gas pressure and temperature increased, the numbers of bonded particles also increased. In particular, the velocity of an in-flight particle in the kinetic gas flow increased with increasing process gas pressure and temperature, according to Eq. (1) [15].

$$v_p = \frac{1}{1/M(\sqrt{M_w/\gamma RT}) + 0.85(\sqrt{D/x}\sqrt{\rho_p/P_0})} \quad (1)$$

where v_p is the particle velocity, M is the local Mach number, γ is the ratio of specific heats of the gas, R is the gas constant

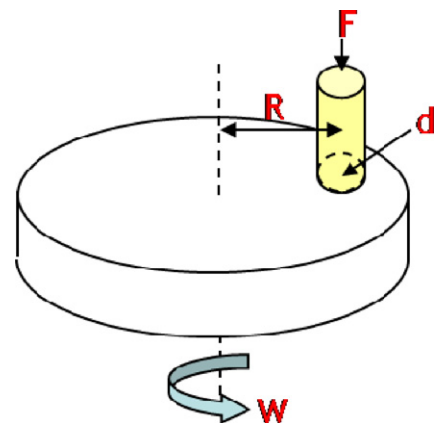
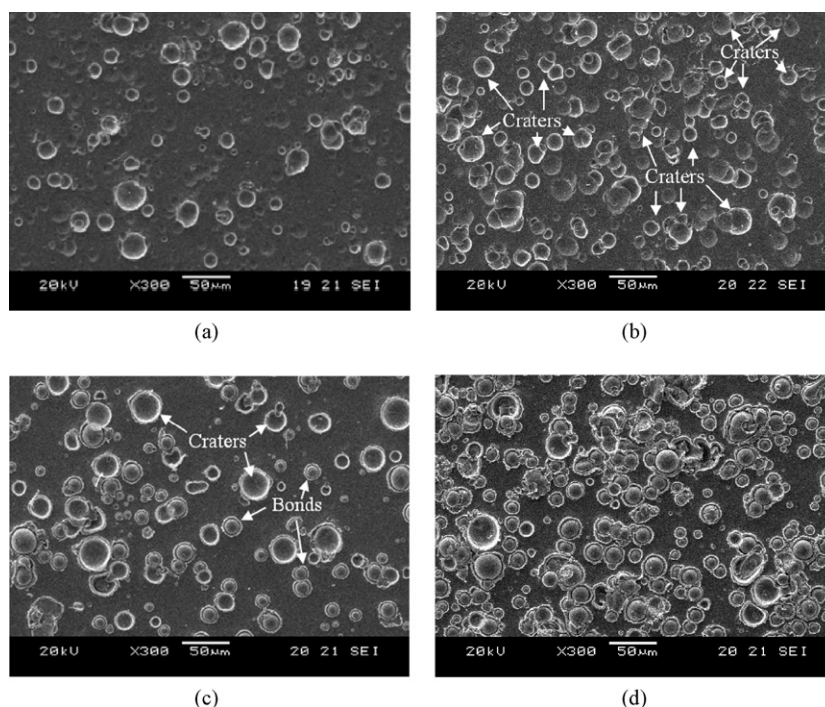


Fig. 2. Schematic of the pin-on-disc dry sliding wear system.

Table 1

Process parameters of the individual impact test.

Feedstock	Process gas type	Process gas pressure (MPa)	Process gas temperature (°C)	Spraying distance
Fe-based BMG	Nitrogen/helium	2.1	350	30 mm
			450	
			550	
		2.5	350	
			450	
			550	
		2.9	350	
			450	
			550	

**Fig. 3.** SEM micrographs of individually impacted and deposited particles at different process conditions: (a) N₂/2.1 MPa/350 °C, (b) N₂/2.9 MPa/550 °C, (c) He/2.1 MPa/350 °C, and (d) He/2.9 MPa/550 °C.

(8314 J kmol⁻¹ K⁻¹), T is the gas temperature, M_w is the molecular weight of the gas, P_0 is the gas pressure measured at the entrance of the nozzle, ρ_p is the particle density, D is the particle diameter, and x is the axial position.

Fig. 4 shows the mean particle velocities determined for all experimental process gas conditions according to Eq. (1). The mean particle velocities when nitrogen was used as the process gas were all lower than the helium case. To estimate the efficiency of particle deposition, the numbers of craters and attached particles were counted. Instead of the deposition efficiency of coatings, the ratio of bonds, which is defined as the fraction of attached particles to total impacted particles (craters + bonds) in a unit area of impact surface, was used in the individual particle impact test. Fig. 5 shows the ratio of bonds under various gas conditions. The results show

that the ratio of bonds tended to increase with the particle velocity only when helium was employed as the process gas. The ratio of bonds had a positive value from 500 m/s and increased to close to 50% at 760 m/s. When a solid particle is impacted onto a planar plate, its deformation behavior is quite dependent on the impacting velocity affecting the strain rate. In fact, there is a certain critical particle velocity in the kinetic spraying above which a particle can be deposited to form a splat, but below which a particle is bounced off. Increase in the particle impacting velocity results in transition of the deformation mode from elastic deformation to plastic flow. Despite the fact that both elastic stress wave propagation and plastic deformation dissipate the kinetic energy of an impacting particle, most of kinetic energy loss results from plastic deformation [7].

Table 2

Process parameters of full coating formation.

Feedstock	Process gas type	Process gas temperature (°C)	Powder preheating temperature	Process gas pressure (MPa)	Spraying distance
Fe-based BMG	Helium	550	Room temperature	2.1	30 mm
				2.5	
				2.9	
				2.1	
			Within $T_g - T_x$	2.5	
				2.9	
				2.9	

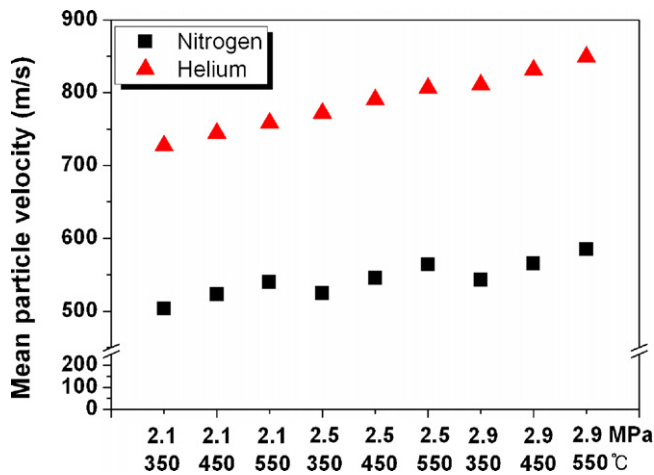


Fig. 4. Calculated mean particle velocity at different process conditions.

Table 3
Conditions for the pin-on-disk wear test.

Materials (specimens)	BMG coating, bearing steel, SBS bearing
Counter part/pin	SUJ2
Pin diameter (<i>d</i>)	5.5 mm
Wear track radius (<i>R</i>)	8 mm
Normal load (<i>F</i>)	100 N
Sliding speed (<i>W</i>)	3 rpm = 15 cm/s
Wear time	600 s
Lubrication	Unlubricated (dry)
Temperature	Room temperature

3.2. Full coating formation

Based on the results of the individual particle impact test, the Fe-based BMG was sprayed for the full coating formation. When nitrogen was used as the process gas, the ratio of bonds was less than 10%, even though the process gas was under high pressure and temperature (2.9 MPa and 550 °C). When helium was used as the process gas, cross-sectional micrographs of as-sprayed BMG coatings for different process gas pressure (process gas temperature was fixed at 550 °C) can be seen in Fig. 6. The coating could be produced, whereas the interparticle bonding features were weakly bonded and slightly deformed, even though the process gas pressure was increased. An impact velocity above 800 m/s was found

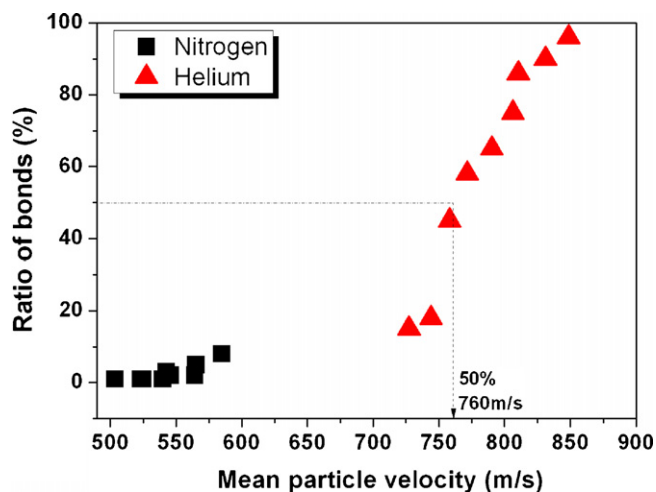


Fig. 5. The ratio of bonds for Fe-based BMG feedstock impacting the substrate at different process conditions.

to be insufficient for the formation of tight bonding of the Fe-based BMG particle. Overall, bare deformation and the resultant weak bonding of the deposited particles can be seen in Fig. 6. It seems that the increased strain and temperature values are insufficient for the formation of strong bonds. The morphology of the splat deposited onto the substrate was different from that of the splat deposited onto the previously deposited overlay. The former is a typical morphology for the hard particle on a soft substrate. Impacting particles were deeply embedded into the substrate. The latter shows severe fractures and weak bonds, mainly due to the characteristics of elastic deformation with some brittle failure under room temperature and a high strain rate. However, any clues of an additional densification effect could not be observed in the coating. This might be due to the elasticity of the BMG material. Compared with the previous research (Ni- [9] and Cu-based [16] BMG coating), Fe-based BMG coating showed a different deposition behavior, and deposition efficiency and density were also relatively lower than those of other BMG coatings, even though the process conditions were the same. In kinetic spraying, the impacting behavior is largely dependent on factors, including the material properties of the particle and the substrate, particle velocity, and impacting angle. The Fe-based BMG has relatively higher melting temperature, hardness, and elastic modulus than Ni- and Cu-based BMG, as shown in Table 4. As a result, a relatively higher energy (kinetic and thermal energy) is required to produce the plastic deformation caused by adiabatic heating at the interface during impact.

It is worth noting that coating formation is largely dependent on gas species and gas conditions, such as gas temperature and pressure. Actually, the impacting particle velocity, a primary factor for BMG particle deposition, is limited due to the brittle nature of the BMG material. Therefore, the kinetic spraying system was modified to increase the deposition efficiency by the formation of more intimate contact at the splat boundary. Considering the effect of the thermomechanical property of the feedstock, an additional heating assembly for heating the powder during the process was designed and attached to the carrier gas line. In this way, dense Fe-based BMG could be deposited.

The Fe-based BMG powder was preheated to 570 °C so that it was within the supercooled liquid region prior to spraying to obtain superplastic deformation upon impact. Cross-sectional micrographs of as-sprayed BMG coatings can be seen in Fig. 7. It can be clearly seen that the particles in the unpreheated case (Fig. 6) were barely and slightly deformed, whereas similar particles in the preheated case (Fig. 7) were more severely deformed. The superplasticity of the particle is initiated during deposition if the temperature reaches the glass transition temperature at the point of impact. As the initial powder is heated, porosity is decreased but maximum thickness of the overlay is increased, compared with the unpreheated case (Fig. 6). With the same feeding rate, the maximum thickness of the overlay can be a qualitative indicator of deposition efficiency. Therefore, the Fe-based BMG particle is more effectively deposited with the additional heating of the initial powder. Notably, the porosity decreased, and the strong bonding formed, due to the enhanced thermal softening resulting from the powder preheating. External thermal energy injection into the system (i.e., an increase in the initial temperature) can change the initial state of the impacting bodies, such as decrease of the flow stress due to thermal softening, based on the Johnson–Cook plasticity model [17].

3.3. Tribological behavior

There is an interest in increasing the applications of BMG for industry. The possibility for the application of Fe-based BMG coating in bearing parts was investigated in this study, with a focus on the wear behavior by the pin-on-disk method at room tempera-

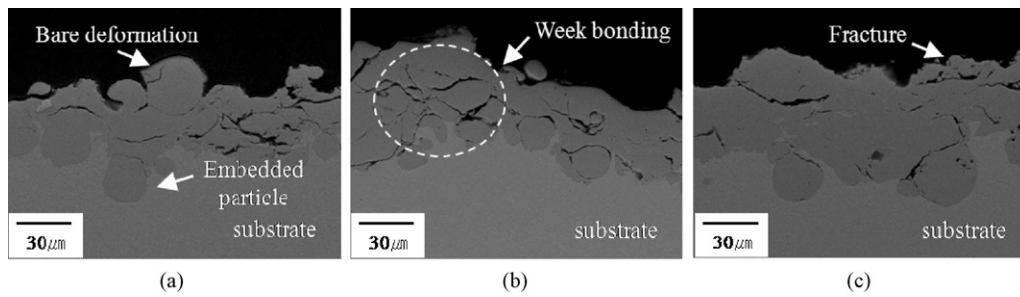


Fig. 6. Cross-sectional micrographs of as-sprayed BMG coatings at different process gas pressures: (a) 2.1 MPa, (b) 2.5 MPa, and (c) 2.9 MPa (constant gas type and process gas temperature, He/550 °C) with unpreheated powder.

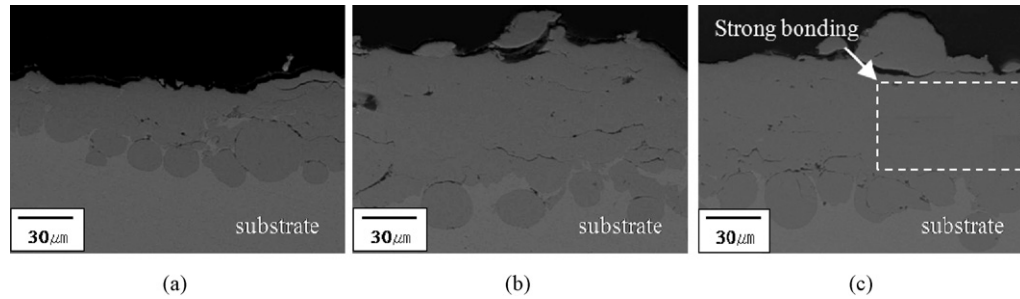


Fig. 7. Cross-sectional micrographs of as-sprayed BMG coatings at different process gas pressures: (a) 2.1 MPa, (b) 2.5 MPa, and (c) 2.9 MPa (constant gas type and process gas temperature, He/550 °C) with powder preheated between T_g and T_x .

ture in comparison with the commercial bearing material, general bearing steel and SBS bearing.

The average microhardness of the Fe-based BMG coating, bearing steel, and SBS bearing was measured and is shown in Fig. 8. Obviously, the as-sprayed coatings exhibited a significantly high hardness, compared with bearing steel and SBS bearing specimen. The high hardness obtained is mainly due to characteristics of the kinetic spray coating process, which are the retained properties

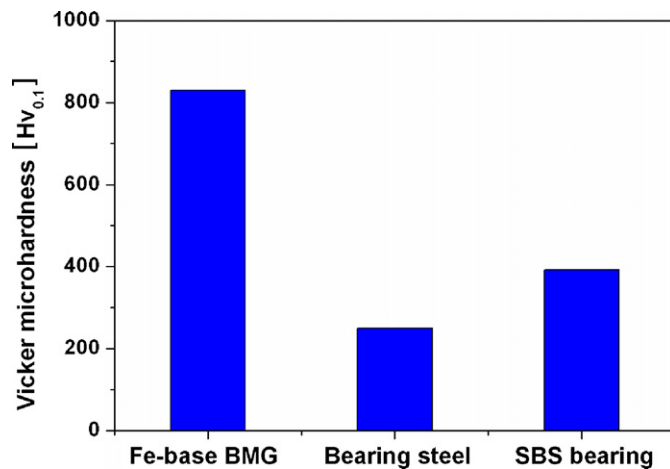


Fig. 8. The average microhardness of the Fe-based BMG coating, bearing steel, and SBS bearing.

Table 4
Thermomechanical properties of bulk metallic glass feedstock.

Feedstock	T_g (°C)	T_x (°C)	T_m (°C)	Nano-indentation hardness (GPa)	Elastic modulus (GPa)
Ni-base BMG	546	597	999	7.0	69.3
Cu-base BMG	439	496	1000	4.9	37.5
Fe-base BMG	539	580	1150	13.6	157.6

T_g : glass transition temperature, T_x : crystallization temperature, T_m : melting temperature.

of the initial particles with additional work hardening [18,19]. It is expected that the wear resistance is generally proportional to the hardness. However, BMG generally shows a different tendency of wear behavior with respect to the hardness. The hardness of the as-sprayed BMG coating can be increased by increasing the crystal fraction of the as-sprayed coating [9]. Meanwhile, in the case of BMG coating, both the friction coefficient and the weight loss were decreased due to the reduction in the ductility and the tensile strength by the crystallization [9]. Also, wear resistance is more affected by the amorphous fraction and microstructure of the as-sprayed coating.

The friction coefficient of the Fe-based BMG coating, bearing steel, and SBS bearing after the wear tests is shown in Fig. 9a. The weight loss of each specimen was calculated from the difference of mass before and after the wear test, which was measured using an electronic balance, as shown in Fig. 9b. It is apparent that SBS bearing specimen exhibits an excellent wear resistance, which is inversely proportional to wear weight loss and is approximately 3 times and 9 times lower than that of the BMG coating and bearing steel, respectively. Fe-based BMG coating also shows a good wear resistance with a low friction coefficient, when compared with a thermal sprayed Fe-based BMG coating case [20].

Fig. 10 shows SEM micrographs of the worn surface of the BMG coating, bearing steel, and SBS bearing. The morphology of the track indicates that BMG coating experienced plastic deformation with grooves and some debris and no visible cracking or fracture after the wear test, as shown in Fig. 10a. Otherwise, the worn surface of the bearing steel specimen is mainly composed of relatively deep grooves and big scars, which caused the rough

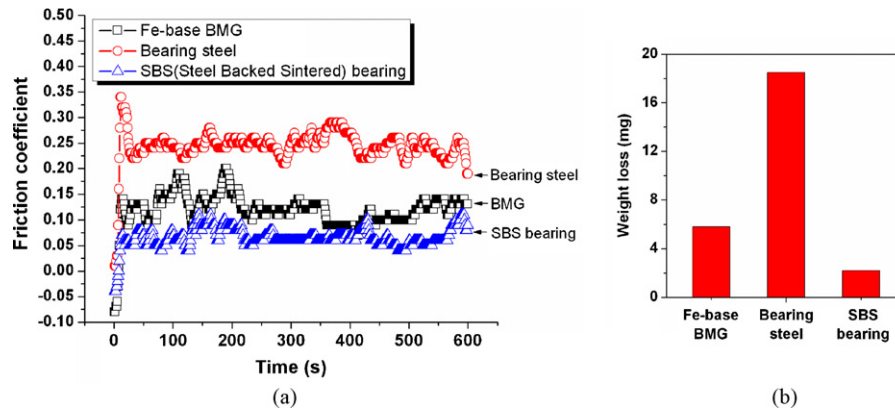


Fig. 9. (a) Friction coefficient and (b) weight loss of the Fe-based BMG coating, bearing steel, and SBS bearing after the wear test.

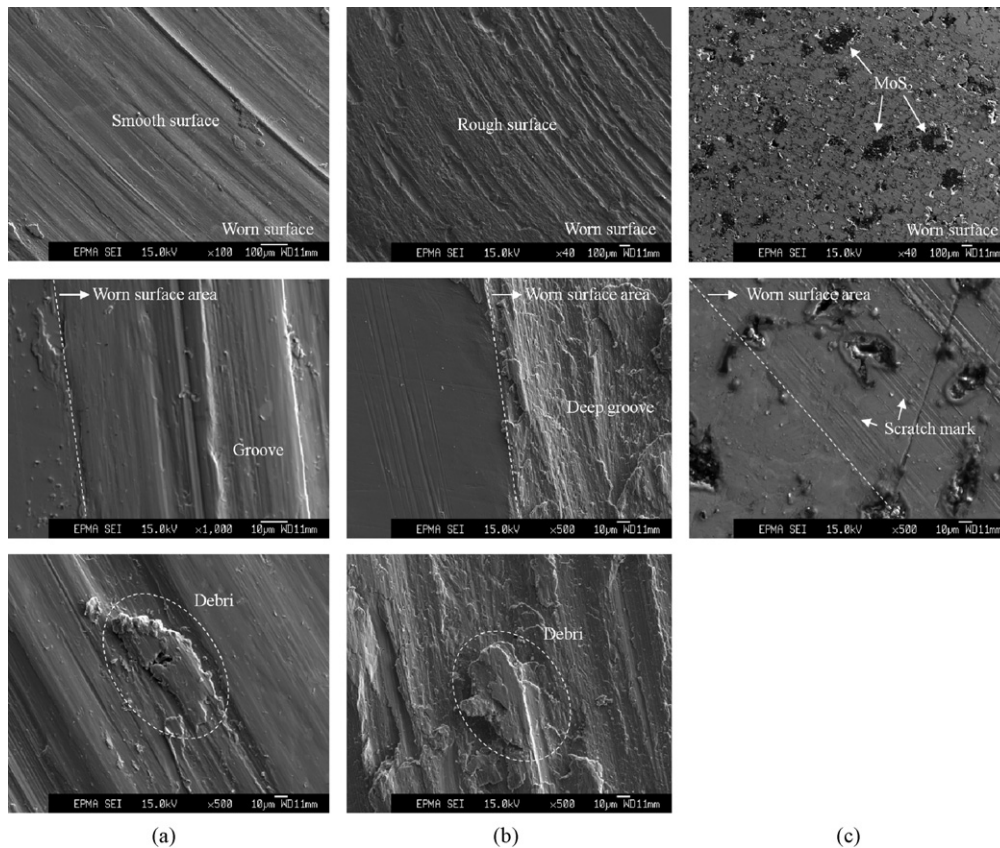


Fig. 10. Worn surface morphologies of: (a) Fe-based BMG coating, (b) bearing steel, and (c) SBS bearing.

surface and increased the friction coefficient and weight loss, as shown in Fig. 10b. However, the worn surface of the SBS bearing specimen shows only a scratch mark, without any visible crack, as shown in Fig. 10c. In the case of the SBS bearing specimen, Fe–Cu materials play an important role as solid lubricants during wear test. MoS₂ particles are also distributed homogeneously in sintered material, which can increase wear resistance and decrease weight loss.

Several investigations of the frictional and wear behavior of BMGs showed different tribological characteristics. Blau [21] reported no evidence for phase transformation on the worn surface. Fu et al. [22], on the other hand, reported that crystallization occurred on the amorphous metallic glass due to friction heating during the wear test, and the crystalline metallic glasses were

also re-amorphized. In the previous study, it has been shown that amorphous phase can be partially transformed to nanocrystalline structure [19]. The pressure- and strain-induced temperature rise might be responsible for the localized crystallization of BMG during the wear test. Some of the worn surface can possibly reach the crystallization temperature. However, most of researchers observed similar plastic deformation patterns on the worn surface due to the friction heating.

4. Conclusions

When helium was used as the process gas, Fe-based BMG coating could be formed via the kinetic spray process. As the powder preheating temperature was increased within the supercooled

liquid region of the BMG for a given same kinetic energy, the particles bonded more tightly with increased deposition efficiency. Notably, the porosity decreased, and the strong bonding occurred due to the enhanced thermal softening resulting from the powder preheating.

Fe-based BMG coating showed a good wear resistance with a low friction coefficient. The worn surface of the Fe-based BMG mainly revealed that the plastic deformation with grooves and some debris were observable with no visible cracking or fracture. It can be concluded that the kinetic spray process is suitable for the formation of Fe-based BMG coating, a potential material for application in bearing parts.

Acknowledgements

This work was financially supported by the Ministry of Knowledge Economy (MKE), Republic of Korea, under the project named development of structural metallic materials and parts with super strength and high performance and the Korea Science and Engineering Foundation (KOSEF) Grant, funded by the Ministry of Science and Technology (MOST), Republic of Korea (no. 2006-02289).

References

- [1] T. Gloriant, J. Non-Cryst. Solids 316 (2003) 96.
- [2] X. Wang, I. Yoshii, A. Inoue, Y.H. Kim, I.B. Kim, Mater. Trans. JIM 40 (1999) 301.
- [3] A. Inoue, B. Shen, C.T. Chang, Acta Mater. 52 (2004) 4093.
- [4] S.J. Pang, T. Zhang, K. Asami, A. Inoue, Corros. Sci. 44 (2002) 1847.
- [5] A. Inoue, A. Makino, T. Mizushima, J. Magn. Magn. Mater. 215–216 (2000) 246.
- [6] J. Kim, K. Kang, S.H. Yoon, S. Kumar, H. Na, C. Lee, Acta Mater. 58 (2010) 952.
- [7] G. Bae, Y. Xiong, S. Kumar, K. Kang, C. Lee, Acta Mater. 56 (2008) 4858.
- [8] H.-B. Jung, J.-I. Park, S.-H. Park, H.-J. Kim, C. Lee, J.-W. Han, Met. Mater. Int. 15 (6) (2009) 967.
- [9] S.H. Yoon, C. Lee, H.S. Choi, Mater. Sci. Eng. A 449–451 (2007) 285.
- [10] B. Jodoin, P. Richer, G. Bérubé, L. Ajdelsztajn, A. Erdi-Betchi, M. Yandouzi, Surf. Coat. Technol. 201 (2007) 7544.
- [11] S.H. Yoon, C. Lee, H.S. Choi, H. Jo, Mater. Sci. Eng. A 415 (2006) 45–52.
- [12] S.H. Yoon, H.J. Kim, C. Lee, Surf. Coat. Technol. 200 (2006) 6022–6029.
- [13] Shinkang, <http://www.shinkang.co.kr/>.
- [14] H. Li, S. Yi, H.S. Sohn, J. Mater. Res. 22 (2007) 164.
- [15] J. Wu, H. Fang, S.H. Yoon, H.J. Kim, C. Lee, Appl. Surf. Sci. 252 (2005) 1368.
- [16] S.H. Yoon, Y. Xiong, H.J. Kim, C. Lee, J. Phys. D: Appl. Phys. 42 (2009) (082004).
- [17] G. Bae, S. Kumar, S.H. Yoon, K. Kang, H. Na, H.J. Kim, C. Lee, Acta Mater. 57 (2009) 5654.
- [18] J.C. Lee, Y.C. Kim, J.P. Ahn, H.S. Kim, S.H. Lee, B.J. Lee, Acta Mater. 52 (2004) 1525.
- [19] S.H. Yoon, G. Bae, Y. Xiong, S. Kumar, K. Kang, J.J. Kim, C. Lee, Acta Mater. 57 (2009) 6191.
- [20] S. Kumar, J.S. Kim, H.J. Kim, C. Lee, J. Alloys Compd. 475 (2009) L9.
- [21] P.J. Blau, Wear 250 (2001) 431.
- [22] X.Y. Fu, T. Kasai, M.L. Falk, D.A. Rigney, Wear 250 (2001) 409.